Construction of rugged, ultrastable optical assemblies with optical component alignment at the few microradian level

Christian J. Killow,* Ewan D. Fitzsimons, James Hough, Michael Perreur-Lloyd, David I. Robertson, Sheila Rowan, and Henry Ward

School of Physics and Astronomy, Scottish Universities Physics Alliance (SUPA), Institute for Gravitational Research, University of Glasgow, Glasgow G12 8QQ, UK

*Corresponding author: Christian.Killow@glasgow.ac.uk

Received 27 September 2012; revised 23 November 2012; accepted 25 November 2012; posted 26 November 2012 (Doc. ID 176989); published 7 January 2013

A method for constructing quasimonolithic, precision-aligned optical assemblies is presented. Hydroxide-catalysis bonding is used, adapted to allow optimization of component fine alignment prior to the bond setting. We demonstrate the technique by bonding a fused silica mirror substrate to a fused silica baseplate. In-plane component placement at the submicrometer level is achieved, resulting in angular control of a reflected laser beam at the sub-10-μrad level. Within the context of the LISA Pathfinder mission, the technique has been demonstrated as suitable for use in space-flight applications. It is expected that there will also be applications in a wide range of areas where accuracy, stability, and strength of optical assemblies are important.

OCIS codes: 220.1140, 220.4610, 120.6085, 120.3180.

1. Introduction

In this article we address the challenges involved in constructing optical assemblies with centimeter-scale reflecting components that are positioned with submicrometer lateral accuracy and microradian angular accuracy. The technique we describe was originally developed for the building of the Laser Interferometer Space Antenna (LISA) Pathfinder optical bench interferometer [1] and is expected to be used in optical bench manufacture for the planned spaceborne gravitational wave detector, eLISA [2,3]. However, the approach is widely transferable to any system requiring precision alignment of laser beams and subsequent stability of laser beam pointing. The technique has the added advantage of now having been space-qualified.

The enabling technology we use is hydroxide-catalysis bonding [4], which we have adapted specifically to be compatible with prebonding adjustable positioning of optical components [5,6]. Hydroxide-catalysis bonding is a well-established technique for joining materials that can form oxide layers and was originally developed in the context of the Gravity Probe B mission [7] and subsequently adapted for use in ground-based gravitational wave detectors [8]. The technique has many characteristics that make it desirable for use in precision optical assemblies, including structural strength, reliability, and the fact that the bond layer can be extremely thin. Hydroxide-catalysis bonding differs from the use of epoxies in that it doesn't involve the addition of significant amounts of material between the two surfaces being joined. This leads to superior dimensional stability and the absence of material that could give rise to outgassing, and hence it is vacuum compatible.

2. Defining the Degrees of Freedom

The coordinate system defined in Fig. 1 will be used to describe the degrees of freedom to be controlled during alignment.

1559-128X/13/020177-05$15.00/0

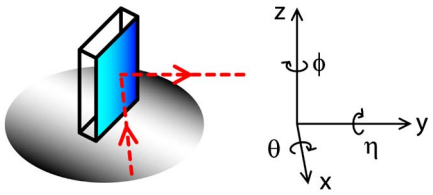

Fig. 1. (Color online) Schematic defining the coordinate system. The dashed line represents the laser beam. The beam enters parallel to the x axis, and the reflected beam is nominally parallel to the y axis.

The approach taken to align a reflected beam to a nominal beam vector is to separately control the "out-of-plane" and "in-plane" degrees of freedom. Here out-of-plane refers to beam position evolution in z. A predetermined value of z is maintained using manufacturing tolerances in partnership with a uniform bond layer. In-plane alignment is achieved by controlling the component position in x and y and angle φ.

3. Bonding Method

The region of the baseplate to which the component will be bonded and the bonding surface of the component are cleaned using a cerium oxide polishing paste, which is subsequently removed using bicarbonate of soda and clean water. Immediately prior to bonding, the surfaces are wiped with methanol that has a low residue on evaporation, which is then allowed to evaporate. Sodium silicate solution is placed on one surface, and the surfaces brought into contact. After approximately 2 min. the bond starts to form, with full strength being reached after four weeks at room temperature.

The bonding surfaces must be suitably conformal for the bonding process to operate as expected: the usual surface geometry specification is that it should be flat to ~60 nm peak-to-valley (commonly stated by optical manufacturers as $\lambda/10$, for λ of 633 nm). This requirement should be met over the full area to be bonded. Ideally the surfaces should be completely smooth, but in practice surfaces that have been polished to a flatness of ~60 nm have been found to have suitable roughness for bonding.

In the case of adjustable bonding, the in-plane alignment process is carried out while the optic is floated on a buffer fluid in order to prevent optical contacting. The buffer fluid used here is octane, which has been chosen for its rate of evaporation and viscosity. Octane with a low residue on evaporation is used to avoid introducing contamination that could affect the bonding process. The component is placed such that it is in contact with ruby balls at the tips of actuated positioners, and the reflected beam is measured with a calibrated target, as described further in Section 5.B. The actuated positioners act as adjustable kinematic stops that define the position of the component. The component is removed and replaced after every movement to ensure it is located against the positioners and periodically removed as the buffer fluid evaporates to allow more to be applied. The alignment is iteratively brought toward the nominal until, in a final step, bonding fluid is applied instead of buffer fluid and the optic replaced. The bonding process used allows approximately 2 min. of fine adjustment before the bond starts to cure, and the component cannot be adjusted further without disturbing the bonding process.

For components requiring lower precision placement, a nonadjustable template can be used in place of the actuated positioners. In the case of template bonding, the kinematic stops are ball bearings mounted in a brass template, and there is no adjustment of the component after it is placed on the baseplate with bonding fluid applied.

15 min. after the bond has started to form, it has cured sufficiently that the locating stops can be removed and the bond left to cure fully.

4. Out-of-Plane Alignment

The lack of any adjustability in the out-of-plane alignment process is a deliberate choice that places requirements on the manufacturing and bonding processes. The out-of-plane alignment is controlled by a combination of factors:

- The flatness of the baseplate, typically specified to be ~160 nm (commonly stated by optical manufacturers as $\lambda/4$, for λ of 633 nm) over 10 cm length scales. This is an alignment requirement and is in addition to the ~60 nm flatness requirement for the bonding process.
- The perpendicularity to the reflecting face of the mirror bonding surface, typically specified to be within 5 μrad.
- The bond layer being either sufficiently thin or at least homogeneous in thickness.

The contributions of these factors are indicated in Fig. 2. The largest expected contribution from a polished baseplate arises from a sinusoidal surface figure with a period equal to the length scale of 10 cm and with 160 nm amplitude. The maximum gradient of this sine wave is then $\pi \times 160 \times 10^{-9}/0.1$, giving an estimate for α of around ±5 μrad. The tolerance on perpendicularity of optical component bonding and reflecting surfaces is $\delta = \pm 5$ μrad. Investigations of bond layer thickness and wedge angle for fused silica are ongoing. Scanning electron microscope investigation of a visibly poor bond with small voids showed a wedge angle, β, of 10 μrad. The wedge angle of a good bond, achievable with careful surface preparation,

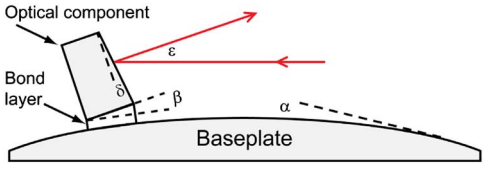

Fig. 2. (Color online) Schematic showing the contributing factors to "out-of-plane" misalignment.

should be significantly smaller, although this is not currently proven.

Taking the worst case values, and assuming these angles are not correlated, we arrive at a root-sum-square value for the component angle with respect to the incoming beam of ~12 μrad, or $\varepsilon \approx 24$ μrad per reflection.

If all the angular deviations added linearly, we could expect $\varepsilon_{\text{worst}} \approx 40$ μrad per reflection, so minimizing systematic effects, for example, in component perpendicularity and bond wedge angle, is important to reduce error buildup after reflections from many components. For transmissive components, lack of parallelism between input and output surfaces can also deviate a beam, and parallelism can also be controlled with few-microradian accuracy.

As a guide to what has been achieved in a system with multiple components bonded to a single baseplate, measurements of out-of-plane deviations have been made on three different beams from the LISA Pathfinder flight model optical bench after each has experienced reflections from multiple bonded mirrors. For the three cases the out-of-plane beam angles were measured to be 43 μrad after four reflections, 36 μrad after five reflections, and 54 μrad after six reflections. Taking the worst case example, that of 54 μrad after six reflections, and assuming that the contributions at each of the four reflections are uncorrelated, then a beam angle deviation per reflection of $54/\sqrt{6}$ or ~22 μrad is deduced, broadly consistent with the value of ε expected.

5. In-Plane Alignment

A. Template Bonding

For components whose positioning requirements are in the tens of micrometers regime, templates and a coordinate measurement machine (CMM) can be used without the need for a laser beam reflected off the component to accurately determine its orientation. This method is described in [9,10], with the results from a larger data set reported here. Figure 3 shows the LISA Pathfinder flight optical bench partway through assembly, with two optical components just having been positioned by template. This shows the three locating ball bearings per component that act as kinematic stops. The substrate to which the components are bonded is inclined at an angle of ~5°, which results in the component resting against the two ball bearings on the long edge that define the reflecting surface angle and position, and the one ball bearing on the short side that ensures the beam will hit the component centrally. Template bonding has the added advantage that several bonds can be made in one bonding session. Once the bonds have partially cured, the template can be backed off and raised on the screws seen in the photograph.

Data from three bonding sessions using different templates to locate two, four, and five optical components showed angular deviations from the nominal for the bonded components of <4 mrad. With the ball bearing separation of ~1 cm, this corresponds to a worst-case relative ball bearing positioning of 40 μm. The same templates were used three times in total, and from this the repeatability of component placement was seen to be <250 μrad. This shows that the angular error observed from the template bonding was dominated by manufacturing tolerances.

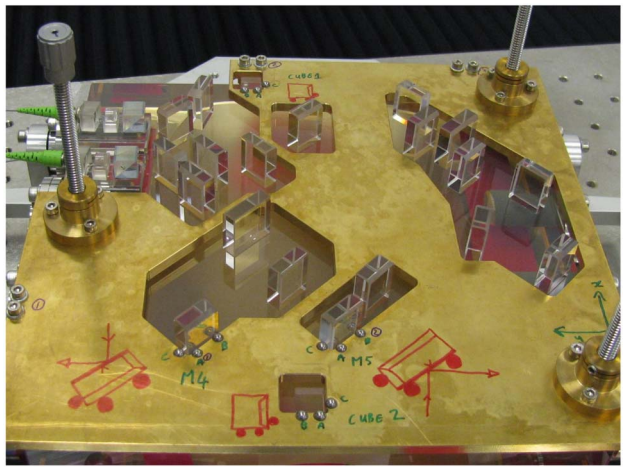

Fig. 3. (Color online) Photograph of a template being used to locate optical components on the LISA Pathfinder optical bench interferometer. Two optical components have just been bonded; they are located next to the labels M4 and M5.

B. Adjustable Bonding

For components with tighter alignment requirements, a reflected beam is used in conjunction with knowledge of the desired beam position and direction derived from a software optical model. In order to align the actual reflected beam as closely as possible to the theoretical beam, an established measurement reference frame and a calibrated target are required. In our case, physical measurements are made by a CMM with an accuracy for each hit point measurement of 1.5 μm + 3 μm/m. Beam vector measurements are made using a target that consists of an Invar structure with a beam splitter and two quadrant photodiodes mounted to it [11]. This device was calibrated such that the coordinate transformation between the physical position of the device as measured by the CMM and the beam vector within the CMM measurement volume was known. With this CMM the optical axis of the target could be determined to ±20 μrad. A LabView [12] front end was designed to read out the beam positions in real time, and a PI H-824 Hexapod was normally used to manipulate the position of the target [13].

Once the CMM measurements of the baseplate have been used to set up the reference frame, the calibrated target is first used as a beam vector measurement tool. By aligning the target using the fine control of the Hexapod actuator on which it is mounted, the input beam is centered on the target's position-sensitive photodetectors; the beam vector can then be derived from CMM measurements of the target. The target is then placed so that its nominal

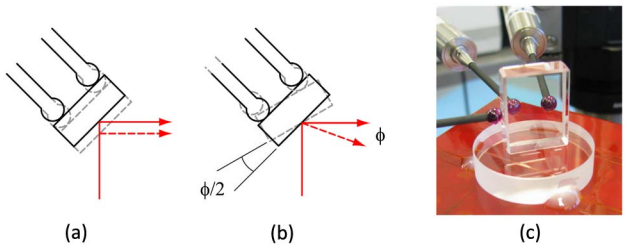

Fig. 4. (Color online) (a) Schematic showing component in-plane lateral adjustment, viewed down the z axis. Solid lines indicate positions prior to adjustment, and dashed lines after adjustment. The arrowed line represents the laser beam vector. (b) Same as (a) but for angular adjustment. (c) Photograph of adjustable positioning of a test optic; the silica baseplate has a diameter of 32 mm.

measurement axis is coincident with that of the desired reflected beam. Live readout of the accuracy of alignment of the component to be bonded is then available.

The actuated positioners that act as kinematic stops to dictate the position of the optic are shown in Fig. 4. The degrees of freedom of the reflected beam controlled during the manipulation and bonding of the mirror to the baseplate are x, y, and φ, as defined in Fig. 1. A common mode movement of both actuated positioners results in the reflected beam undergoing a lateral translation (no angular deviation) of $1/\sqrt{2}$ times the component movement. A differential movement of the actuators results in a change in φ. For a typical positioner separation at the component of 10 mm, moving the positioners by 1 μm each, in different directions, results in an angular movement of the optic of 200 μrad and a change in φ of 400 μrad. There will also be an additional lateral shift if the beam is not incident at the center of rotation.

In Fig. 4(c) the baseplate is placed at a slight angle in order that gravity assists in locating the component against the positioners when it is floating either on a temporary buffer fluid or on the final bonding fluid. The third positioner is located so as to constrain movement of the component in the plane of the reflecting surface.

The data in the plot shown in Fig. 5 were taken during the alignment and bonding of this test mirror. In this demonstration of the technique the goal was to center the beam simultaneously on the two quadrant photodiodes in the target. These photodiodes were located 22 and 71 cm from the mirror to be bonded. The plot shows a time series of the in-plane positions of the reflected beam. The coarse alignment, prior to 1400 s, is not shown, and the breaks in the data correspond to the component being moved for resettling, the application of more buffer fluid, or the application of bonding fluid. The trace for the far photodiode is noisier than that for the near photodiode due to the beam having travelled farther in turbulent air.

Some points of interest labeled on the plot are:

A. Removal of the mirror to replenish the buffer fluid.

B. Removal of the mirror for bonding fluid application.

C. Replacement of the mirror and the start of the bonding process.

D. Final adjustment of the mirror before leaving the bond to cure.

The expanded plot showing the time period ~1800–2075 s demonstrates the level of repeatability when removing and replacing the component on buffer fluid. The movement as it settles is due to the relatively thick buffer fluid layer allowing the component to settle out-of-plane, which has a cross coupling into the in-plane reading. This leads to some uncertainty as to where the component will settle when the buffer fluid is replaced with bonding fluid, but this is recoverable using the range of possible adjustment once the bonding fluid has been applied.

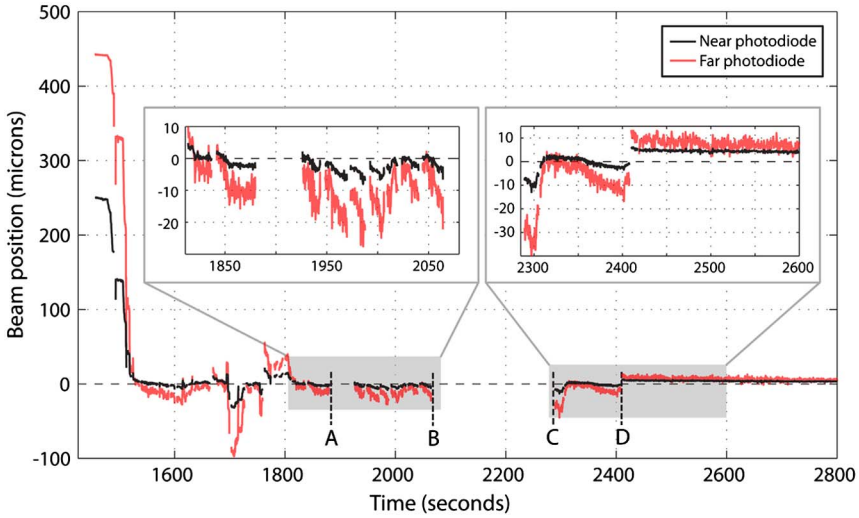

Fig. 5. (Color online) Graph showing the in-plane positions of the laser beam at the near and far photodiodes during the final alignment and bonding stages of the mirror.

Table 1. Summary of Demonstrated Alignment Accuracies

	Alignment Achieved (microradians)
Out-of-plane	22
In-plane—template absolute	<4000
In-plane—template repeatability	<250
In-plane adjustable	6

The expanded plot from ~2300–2600 s shows the alignment immediately before the bond starts to cure. The effects of small adjustments of the actuator positioners and subsequent encouragement of the component to rest against the ruby balls can be seen.

The final beam offsets at the near and far photodiodes were 5 and 8 μm. This represents an in-plane angle from the nominal goal vector of ~6 μrad. This is a typical level of accuracy achievable using current techniques. The last adjustment of the positioning actuator, at point D, changed the photodiode spot positions from −2 to −7.5 μm (corresponding to −11 μrad offset) to 5 and 8 μm; the total angular change resulting from the movement was thus 17 μrad. Since the actuators are separated by 11 mm, this level of position control of the mirror corresponds to a differential actuator movement of ~0.1 μm. The achieved accuracies for all methods of alignment demonstrated are summarized in Table 1.

6. Conclusions

A technique for precision bonding of optical components to a substrate using a chemical process previously shown to exhibit picometer stability has been presented. This technique has many useful characteristics—it is mechanically strong, provides bonds that are thin and vacuum compatible, and, crucially, allows fine optimization of the component positioning both prior to and during the bonding process. Bonding of centimeter-scale optics with micrometer-level precision of positioning has been demonstrated.

This research was supported through awards from the UK Science and Technologies Facilities Council (STFC), the United Kingdom Space Agency (UKSA), and the University of Glasgow. C. Killow wishes to acknowledge support from the Scottish Universities Physics Alliance.

References

1. F. Antonucci, M. Armano, H. Audley, G. Auger, M. Benedetti, P. Binetruy, C. Boatella, J. Bogenstahl, D. Bortoluzzi, P. Bosetti, M. Caleno, A. Cavalleri, M. Cesa, M. Chmeissani, G. Ciani, A. Conchillo, G. Congedo, I. Cristofolini, M. Cruise, K. Danzmann, F. De Marchi, M. Diaz-Aguilo, I. Diepholz, G. Dixon, R. Dolesi, N. Dunbar, J. Fauste, L. Ferraioli, D. Fertin, W. Fichter, E. Fitzsimons, M. Freschi, A. G. Marin, C. G. Marirrodriga, R. Gerndt, L. Gesa, F. Gilbert, D. Giardini, C. Grimani, A. Grynagier, B. Guillaume, F. Guzmán, I. Harrison, G. Heinzel, M. Hewitson, D. Hollington, J. Hough, D. Hoyland, M. Hueller, J. Huesler, O. Jeannin, O. Jennrich, P. Jetzer, B. Johlander, C. Killow, X. Llamas, I. Lloro, A. Lobo, R. Maarschalkerweerd, S. Madden, D. Mance, I. Mateos, P. W. McNamara, J. Mendes, E. Mitchell, A. Monsky, D. Nicolini, D. Nicolodi, M. Nofrarias, F. Pedersen, M. Perreur-Lloyd, A. Perreca, E. Plagno, P. Prat, G. D. Racca, B. Rais, J. Ramos-Castro, J. Reiche, J. A. R. Perez, D. Robertson, H. Rozemeijer, J. Sanjuan, A. Schleicher, M. Schulte, D. Shaul, L. Stagnaro, S. Strandmoe, F. Steier, T. J. Sumner, A. Taylor, D. Texier, C. Trenkel, D. Tombolato, S. Vitale, G. Wanner, H. Ward, S. Waschke, P. Wass, W. J. Weber, and P. Zweifel, "LISA pathfinder: mission and status," Class. Quantum Grav. **28**, 094001 (2011).
2. LISA International Science Team, "LISA: unveiling a hidden universe," Assessment Study Report ESA/SRE(2011)/3 (European Space Agency, 2011).
3. P. Amaro-Seoane, S. Aoudia, S. Babak, P. Binétruy, E. Berti, A. Bohé, C. Caprini, M. Colpi, N. J. Cornish, K. Danzmann, J.-F. Dufaux, J. Gair, O. Jennrich, P. Jetzer, A. Klein, R. N. Lang, A. O. Lobo, T. Littenberg, S. T. McWilliams, G. Nelemans, A. Petiteau, E. K. Porter, B. F. Schutz, A. Sesana, R. Stebbins, T. Sumner, M. Vallisneri, S. Vitale, M. Volonteri, and H. Ward, "Low-frequency gravitational-wave science with eLISA/NGO," Class. Quantum Grav. **29**, 124016 (2012).
4. D.-H. Gwo, "Ultra-precision and reliable bonding method," U.S. patent 6,284,085 B1 (4 September 2001).
5. E. J. Elliffe, J. Bogenstahl, A. Deshpande, J. Hough, C. Killow, S. Reid, D. Robertson, S. Rowan, H. Ward, and G. Cagnoli, "Hydroxide-catalysis bonding for stable optical systems for space," Class. Quantum Grav. **22**, S257–S267 (2005).
6. D. Robertson, C. Killow, H. Ward, J. Hough, G. Heinzel, A. Garcia, V. Wand, U. Johann, and C. Braxmaier, "LTP interferometer—noise sources and performance," Class. Quantum Grav. **22**, S155–S163 (2005).
7. C. W. F. Everitt, D. B. DeBra, B. W. Parkinson, J. P. Turneaure, J. W. Conklin, M. I. Heifetz, G. M. Keiser, A. S. Silbergleit, T. Holmes, J. Kolodziejczak, M. Al-Meshari, J. C. Mester, B. Muhlfelder, V. G. Solomonik, K. Stahl, P. W. Worden, Jr., W. Bencze, S. Buchman, B. Clarke, A. Al-Jadaan, H. Al-Jibreen, J. Li, J. A. Lipa, J. M. Lockhart, B. Al-Suwaidan, M. Taber, and S. Wang, "Gravity probe B: final results of a space experiment to test general relativity," Phys. Rev. Lett. **106**, 221101 (2011).
8. J. Hough, "Long baseline gravitational wave detectors—status and developments," Prog. Part. Nucl. Phys. **66**, 233–238 (2011).
9. E. D. Fitzsimons, J. Bogenstahl, J. Hough, C. Killow, M. Perreur-Lloyd, D. I. Robertson, S. Rowan, and H. Ward, "Initial interferometric pre-investigations for LISA," J. Phys. Conf. Ser. **154**, 012034 (2009).
10. E. D. Fitzsimons, "Techniques for precision interferometry in space," Ph.D. thesis (University of Glasgow, 2010).
11. E. D. Fitzsimons, J. Bogenstahl, J. Hough, C. J. Killow, M. Perreur-Lloyd, D. I. Robertson, and H. Ward are preparing a manuscript to be called "Precision absolute positional measurement of laser beams."
12. Labview System Design Software, http://www.ni.com/labview/.
13. Physik Instrumente Hexapods, http://www.hexapods.net/.